Cluster birth–death processes in a vapor at equilibrium

Rodrigo Soto[a] and Patricio Cordero
Departamento de Física, Facultad de Ciencias Físicas y Matemáticas, Universidad de Chile, Casilla 487-3, Santiago, Chile

(Received 23 October 1998; accepted 13 January 1999)

A method is presented to analyze and observe, in molecular dynamic simulations, the statistical properties of instantaneous cluster transitions, mainly fusions and fissions for a homogeneous vapor at equilibrium. The method yields the way to obtain mean lives, branching ratios and, to some extent, transition rates as well. To the best of our knowledge branching rations in cluster decays have not been measured before (simulationally or experimentally). An application of this method to a model system provides a critical reassessment of the standard Homogeneous Nucleation Theory (HNT). Our own simulations show that transitions different from absorbing or evaporating a monomer are quite important, representing in some cases 50% of all decay events. Our method also shows unequivocally that the decay processes involving clusters classified by size alone are not Markovian. © *1999 American Institute of Physics.* [S0021-9606(99)51914-4]

I. INTRODUCTION

Dilute gases near the coexistence line spontaneously create microscopic liquid droplets (*clusters*). If the gas is at equilibrium, there is a permanent presence of clusters because, even though the clusters have a finite mean life and tend to evaporate, new ones are being permanently created. A gaseous system with dynamics influenced by the presence of cluster is called *vapor*. The generally accepted theoretical framework describes vapors in terms of the clusters present in it and the different reactions between clusters.

A cluster dynamic model should describe the cluster reactions as a set of incoming clusters that react producing emerging clusters. All the intermediate steps (the reaction itself) should not be considered. The simplest reactions would be fissions (two or more clusters merge) or fusions (a cluster divides into sub-clusters). Also more complicated reactions can occur. For example, a collision of two clusters typically gives rise to sub-clusters. In our simulations the cluster reactions that cannot be classified as fissions or fusions represent at most 7% of the total number of reactions.

But even in a dilute vapor it is impossible to isolate these processes since the time scales involved in the reactions are comparable with the cluster mean lives and flight times. That is, there are no asymptotic free states that could be associated to the reactants or the products, and it is not clear the instants a reaction starts or ends. As an illustration, the history of a cluster produced in a fusion is presented in Fig. 1. The figure illustrates that there are no clear definitions of which are the intermediate steps and which are the final products.

To avoid ambiguities, the approach we will use in this work is to consider as relevant all microscopic cluster reactions even if they are just intermediate steps. That is, all instantaneous branchings in Fig. 1 are analyzed. Any other choice would lead to ambiguities.

The most successful theory that describes a vapor using cluster dynamics is the Homogeneous Nucleation Theory, HNT.[1–5] This theory describes the evolution of the cluster populations in terms of equilibrium properties and basic kinetic assumptions. The HNT assumes that the only relevant processes are absorption and evaporation of monomers, namely, it assumes that when a cluster changes size it does so changing one step at a time. The theory also assumes that all these processes are Markovian, and the corresponding transition rates depend only on the cluster concentrations, temperature and pressure [see the comments before and after Eq. (7.6) in Ref. 4.]

Since the HNT assumes that all processes change size one step up or down, it is natural to call them fusions or fissions, respectively, and such classification is exhaustive in that case.

The absorption (fusion) transition rates are expressed as the product of the collision rate between clusters and monomers and the *sticking coefficient*. The latter is a measure of the fraction of collisions that are successful, namely, the reactions in which the monomer is actually absorbed by the cluster. Since this coefficient is quite difficult to estimate from a microscopic model several phenomenological models have been put forward.[6,7] Models have been advanced to incorporate the internal degrees of freedom.[8,9] But, usually the sticking coefficient is set to one, which corresponds to considering relevant all microscopic cluster reactions.

To calculate the evaporation (fission) transition rates, the HNT uses detailed balance arguments and the fact that absorption and evaporation are at equilibrium at the saturation pressure.[10–12] The equilibrium concentration of clusters of size k, $N_k(t)/N$, at the saturation pressure are obtained from the so called *capillary approximation* that uses a thermodynamic approach, calculating the concentrations in terms of the cluster's free energy ΔG_k. This free energy is expressed as a sum of a volumetric term and a surface term.

With these assumptions, the HNT gives a set of closed equations for the evolution of the cluster populations which

[a]Present address: CECAM, ENS-Lyon, 46 Allée d'Italie, 69007 Lyon, France; electronic mail: rsoto@cecam.fr

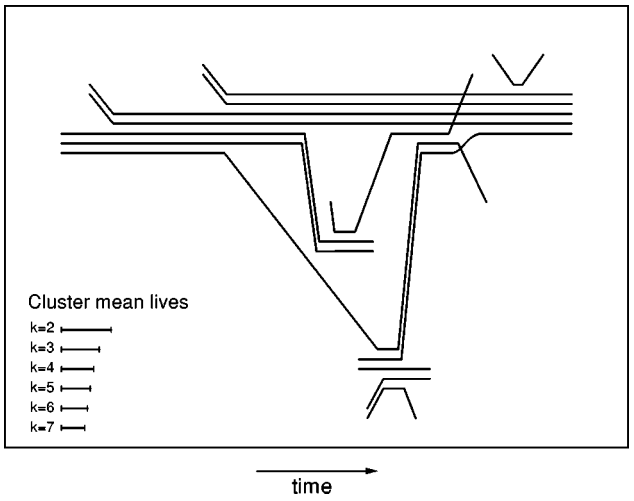

FIG. 1. The schematic history of a cluster of size $k=5$ produced in a fusion of two clusters in a chain of processes actually observed in a simulation. The cluster absorbs, evaporates and re-absorbs particles and sub-clusters in a complicated fashion. As a comparison, the mean lives for clusters of size $k=2$ to $k=7$ are shown. The simulation is at $T=0.68$ and $n=0.05$ and the cluster definition is geometric.

are local in time. From the equations it follows that if the system was placed in a phase space zone where the liquid phase is stable then the same type of dynamics of cluster formation persists with the difference that now the clusters of a size larger than a certain threshold (critical cluster size) grow until macroscopic liquid droplets are formed. The supercritical clusters are produced when a small cluster absorbs sequentially a sufficient number of monomers. Since the HNT assumes that clusters can absorb only monomers and evaporation is more probable than absorption, the above process is slow. The predictions that stem from these equations are mostly successful but in some cases their predictions fail with respect to experiments.[12–16]

Great efforts have been made to improve the classical theory. These efforts have mainly gone in the direction of modifying the free energy calculation (see Ref. 17 and references therein). In Ref. 17 there is a detailed analysis and derivation of the cluster concentrations using a formal virial expansion, and it is found that nonideal corrections to the free energy and pressure are needed to have better predictions.

The HNT has also been reformulated to allow for other decay modes, different from the pure absorption and evaporation of monomers,[18,9,7] introducing appropriate transition rates, which are estimated phenomenologically.

Even though the HNT extensively uses the concept of clusters there is no unique definition for them. The only indication is that clusters are microscopic domains of the liquid phase.[19,4] Usually a cluster is understood either as a set of molecules that are nearer to each other than a specified distance[20] or as a set of molecules inside a spherical shell,[21] or a density fluctuation which exceeds a certain threshold.[22] One can also require that, besides proximity, the particles satisfy some energy requirement associated to the idea of forming a bound state.[23,24] These energetic clusters were proposed as better candidates to have a dynamic theory of vapors, but they have nonclassical kinetic properties. For example, at equilibrium their velocity distribution function is not Maxwellian.

In this paper we study the HNT cluster reactions hypotheses using molecular dynamic simulations for generalized contour clusters.[9,4,17] In Sec. II we present two cluster definitions to work with. In Sec. III we introduce a probabilistic formalism to analyze cluster reactions and a new method that simplifies the measurement of the reaction probabilistic properties in molecular dynamics simulations giving direct access to some quantities needed in HNT. In Sec. IV the method is used to analyze the cluster reactions in molecular dynamics simulations of a vapor model in two dimensions. We find that these processes are not at all Markovian for one cluster definition—geometric—but for another definition—energetic—the processes are closer to being Markovian (in a sense specified later). Further, we measure the branching ratios of the different decay modes associated to several size clusters, which as far as we know have not been measured before. It is found that clusters do not only decay through the absorption or evaporation of monomers. The other modes can be as important as 50% of the total decays. Finally, conclusions are in Sec. V.

II. CLUSTER DEFINITION

Microscopically a vapor will be considered as a nonideal gas mixture in which each species of clusters has a set of internal degrees of freedom. For the sake of simplicity we are going to consider a system made up of point ''molecules'' that simply have translational degrees of freedom and interact with short range potentials.

A cluster will be considered to be a set of particles that in some sense are bound together. For the moment, and without having to provide a detailed definition, it will suffice to use a function $C(\mathbf{r},\mathbf{v})$—that depends on the relative positions and velocities of two particles—of short range in positions, such that C is either 1 or 0 with a well defined criterion. To define clusters we introduce the concept of *linked* particles as follows.

(i) If $C(\mathbf{r_{ab}},\mathbf{v_{ab}})=1$ then by definition *a* and *b* are *linked*; (ii) if particle *a* is linked to *b* and *b* is linked to *c*, then *a* and *c* are linked. Finally, *two particles belong to the same cluster if and only if they are linked.*

Using this generic definition each microscopic state has a unique decomposition in clusters. Contour clusters[20] correspond to choosing $C(\mathbf{r},\mathbf{v})=\Theta(r_0-r)$, where Θ is the Heaviside function. That is, two particles are said to be linked if they are closer than r_0. We will refer to these as *geometric clusters.*

We will also use another definition: *energetic clusters*. Two particles are linked if they are energetically bound, that is,

$$C(\mathbf{r},\mathbf{v})=\Theta\left(\varphi^{\mathrm{eff}}(r_M)-\varphi(r)-\frac{mv^2}{4}\right)\Theta(r_M-r), \qquad (1)$$

where φ is the interparticle potential, φ^{eff} is the effective central potential (centrifugal barrier included), and r_M is the

point where the effective potential is maximum for a given relative angular momentum. A discussion of the properties of these clusters is in Refs. 23,24.

Given any microscopic definition of clusters, the instant when a particular cluster decays corresponds to the instant when it changes microscopically. As a consequence of each one of these processes new clusters are born, and in this sense it can be said that the instants of decay and birth of clusters coincide.

III. PROBABILISTIC ANALYSIS

In this section we describe the basic concepts that appear in the measurement of the probabilistic properties of decay processes. In doing so we use a generic cluster size k throughout this section, and to make the notation simpler we omit the label k from all the quantities we define below.

A. Decay probabilities

Let us assume that, in a vapor at equilibrium, a cluster of size k is created (in the sense given in the previous section) at time $t=0$. There is a probability $p_0(t)dt$ that the cluster will decay in the interval dt after time t. The decay can occur in different modes that we label ℓ. The specific definition of decay modes is arbitrary and it is possible to have a continuous or discrete classification of modes, the only restriction being that the classification covers all possible cases. If the cluster decays at time t, there is a probability distribution $f_\ell(t)$ that the decay occurs through mode ℓ, with $\Sigma_\ell f_\ell(t)=1$. Then,

$$p_0(t)=p_0(t)\sum_\ell f_\ell(t)=\sum_\ell p_{0\ell}(t), \tag{2}$$

where $p_{0\ell}(t)$ is the probability density that at time t a cluster decays through mode ℓ.

At equilibrium, the distributions $p_{0\ell}(t)$ have to be well defined and stationary, independent of the clock time, but dependent on the time lapse t the cluster has lived.

Different statistical properties can be calculated from the distributions $p_{0\ell}(t)$. The mean life of clusters (of size k) is

$$\tau=\int_0^\infty p_0(t)t\,dt. \tag{3}$$

The branching ratio, f_ℓ, through mode ℓ is defined as the probability that the cluster decays through this mode, irrespective of the decay time. That is,

$$f_\ell=\int_0^\infty p_{0\ell}(t)dt. \tag{4}$$

Finally, to study the memory effects in a particular mode we define the transition rate $T_\ell(t)$ as

$$T_\ell(t)=\frac{p_{0\ell}(t)}{1-\int_0^t p_0(s)ds}=\frac{p_{0\ell}(t)}{\int_t^\infty p_0(s)ds}. \tag{5}$$

In other words, $T_\ell(t)$ is the conditional probability that the cluster will decay through mode ℓ in the interval $(t,t+dt)$ given that until t it had not yet decayed.

Several properties of the probability density can be obtained from the transition rates. In particular, if a process is Markovian, the transition rate is constant, but, in general, memory effects appear in the transition rates.

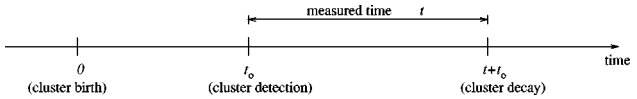

FIG. 2. The times involved in the measurement of the life span of a cluster. The time variable is set to $t=0$ at the unknown instant when the cluster is created.

Similarly, the total transition rate $T(t)$ is defined as

$$T(t)=\frac{p_0(t)}{\int_t^\infty p_0(s)ds}. \tag{6}$$

Therefore, we have shown that the main properties of decay processes can be studied in terms of $p_{0\ell}(t)$. In the next section we derive a procedure to measure these distributions in molecular dynamic simulations.

B. Measured distributions

In principle, if clusters could be detected in the simulation from the time of their creation, they could be followed until their decay, recording their lifetime and decay modes. The distributions $p_{0\ell}(t)$ could be obtained making histograms of the times obtained, classified by mode. In practice, however, it is almost impossible to follow all particles in a simulation until a cluster is created. If only a set of particles were followed, most probably they would participate in small clusters (due to the great fraction of small clusters), preventing us from getting enough statistics in connection with the larger ones.

The approach we use is to take regular snapshots of the system and detecting in them one cluster of each size until a maximum size k. Then, these clusters' histories are followed until they decay, recording in each case the size of the original cluster, the time they lived from detection to decay and the corresponding decay mode. In the next snapshot only clusters of sizes that already decayed are looked for. The ones that still live continue being followed.

As a result of the simulation a list of decay times and decay modes $\{(t_i,\ell_i)\}_{i=1\cdots M}$ are obtained for each cluster size. Assuming that the instants clusters are detected (the snapshots) are uncorrelated from the instants the clusters were created, it follows that the pairs $\{(t_i,\ell_i)\}_{i=1\cdots M}$ are not distributed with $p_{0\ell}(t)$ but with a different distribution $p_\ell(t)$. The distribution $p_\ell(t)$ is the probability density that a cluster will die through mode ℓ a time t after detection regardless of the age t_0 it had at detection. The values t_0 can take are unknown but, since the detection is at random, they are distributed according to the age distribution $p_e(t)$. A graphical description of the times used is given in Fig. 2. In brief, then, $p_\ell(t)$ represents the conditional probability that a cluster decays at time $t+t_0$ given that it has not decayed until t_0, averaged over $p_e(t_0)$,

$$p_\ell(t)=\left\langle \frac{p_{0\ell}(t+t_0)}{1-\int_0^{t_0}p_0(s)ds}\right\rangle_{p_e(t_0)}=\int_0^\infty \frac{p_{0\ell}(t+t_0)}{\int_{t_0}^\infty p_0(s)ds}p_e(t_0)dt_0. \tag{7}$$

We also define $p(t)$ as the probability distribution of the times $\{t_i\}$ irrespective of the decay mode,

$$p(t)=\sum_{\ell} p_{\ell}(t). \tag{8}$$

Expression (7) can be simplified if the age distribution is given in terms of $p_0(t)$. A detailed analysis of the statistical death probability yields

$$p_e(t)=\frac{\int_t^{\infty} p_0(s)ds}{\int_0^{\infty} s p_0(s)ds}. \tag{9}$$

Replacing (9) in (7) gives

$$p_{\ell}(t)=\frac{\int_0^{\infty} p_{0\ell}(t+t_0)dt_0}{\int_0^{\infty} s p_0(s)ds}=\frac{\int_t^{\infty} p_{0\ell}(s)ds}{\int_0^{\infty} s p_0(s)ds}. \tag{10}$$

It is necessary to calculate the factor $\int_0^{\infty} s p_0(s)ds$ to be able to invert the previous relation and thus calculate the distribution $p_{0\ell}$ from the measured distribution p_{ℓ}. Carrying a sum over ℓ on both sides of (10) and evaluating the result at $t=0$ implies

$$\int_0^{\infty} s p_0(s)ds = 1/p(0). \tag{11}$$

Differentiating (10) with respect to t, the inverse relation follows:

$$p_{0\ell}(t)=-\frac{p'_{\ell}(t)}{p(0)}. \tag{12}$$

From definition (2), the probabilities $f_{\ell}(t)$ are

$$f_{\ell}(t)=\frac{p'_{\ell}(t)}{p'(t)}. \tag{13}$$

In terms of the measured distributions $p_{\ell}(t)$, the mean life, branching ratios and transition rates are

$$\tau=\frac{1}{p(0)}, \tag{14}$$

$$f_{\ell}=\frac{p_{\ell}(0)}{p(0)}, \tag{15}$$

$$T_{\ell}(t)=-\frac{p'_{\ell}(t)}{p(t)}, \tag{16}$$

$$T(t)=-\frac{p'(t)}{p(t)}. \tag{17}$$

What we have achieved, then, is to find the way to evaluate physically interesting properties of the decay processes directly from the distributions $p_{\ell}(t)$ that can economically and directly be measured in the simulations.

IV. MOLECULAR DYNAMIC SIMULATIONS

We have made molecular dynamic simulations of a two dimensional vapor at equilibrium (gaseous phase). Our system is a gas of particles that interact with a square well potential φ,

$$\varphi(r)=\begin{cases}\infty & r<\sigma,\\ -\varepsilon & \sigma<r<\alpha\sigma,\\ 0 & \alpha\sigma<r.\end{cases} \tag{18}$$

The units chosen are such that $m=1$, $\varepsilon=1$, $\sigma=1$, and we have set $\alpha=1.5$. The Boltzmann constant is set to one, such that temperatures are given in units of the well depth ε.

We simulated systems of $N=10^3$ particles at temperatures and number densities n corresponding to the pure homogeneous gas phase with a non negligible presence of clusters. The boundary conditions used were periodic to avoid heterogeneous condensation. Systems like this one are known to relax to a state totally independent of the details of the initial condition.

In the case of piecewise constant potentials like (18) the simulation is carried out by the Event Driven Molecular Dynamics technique that, instead of numerically integrating Newton's dynamics, makes the system advance analytically from *event to event*. An event is the instant when two particles meet at a distance equal to a discontinuous change of the potential.[25–27]

After relaxation a first snapshot is taken and one cluster of each size—up to a certain limit ($k=10$)—are looked for. It may happen that no clusters are found of a given size. Right after the snapshot the system is followed from event to event detecting if any of the marked clusters change. If so, the time lapse from detection to this decay and the specific decay mode are recorded. At regular intervals Δt new snapshots are taken. In each snapshot the system is searched for new clusters of sizes that have already decayed and also of sizes for which no specimen was recorded last time. The interval Δt is taken larger than the longest cluster mean life in order to obtain uncorrelated measurements.

Instead of calculating the distribution probabilities $p_{\ell}(t)$ making histograms, since it is too noisy, the lists of times are processed constructing the accumulated probability functions $Q_{\ell}(t)$ and $Q(t)$,

$$Q_{\ell}(t)=\int_0^t p_{\ell}(t)dt, \tag{19}$$

$$Q(t)=\int_0^t p(t)dt. \tag{20}$$

After smoothing these functions a numerical determination of the distributions is easier.

The mode classification is made annotating the sizes of the clusters where the particles of the original cluster now belong. If the cluster under study absorbs another one, then only one size larger than the original size is recorded. Isolated particles are considered clusters of size 1.

Among all possible decay modes most decays could be classified as (a) fusions, namely processes where two or more colliding clusters produce a bigger one or (b) spontaneous fissions, namely, processes where a cluster breaks up without combining its particles with those of another cluster. Spontaneous fissions are detected because the total number of particles in the products is equal to the size of the original cluster; these processes are labeled by the size of the largest product. Fusions are recognized because there is only one

TABLE I. Densities and temperatures used to measure mean lives, transition rates and channel decay fractions. As a reference, the critical density and temperature for this system are $n_c=0.3$ and $T_c=0.8$ (Ref. 28).

Simulation	n	T
Sim 1	0.005	0.68
Sim 2	0.050	0.68

final cluster and its size is larger than the original one; these processes are labeled with the size of the resulting cluster.

In the case of energetic clusters there are other processes besides fissions and fusions, such as the substitution of one particle in the cluster by a colliding monomer or when a trimer collides with a monomer producing two dimers. These are two examples of processes that cannot be classified using the above scheme. With the geometric definition of a cluster, the previous criteria classify all decay modes. In particular, fissions imply exactly two final clusters.

The simulations were made with global density n and temperature T given in Table I. In both cases the system is purely gaseous and the temperature is below the critical temperature.

A. Mean lives

In Fig. 3 the measured mean life for different cluster sizes is shown for geometric and energetic clusters. In terms of the accumulated probability $Q(t)$, the cluster mean life is

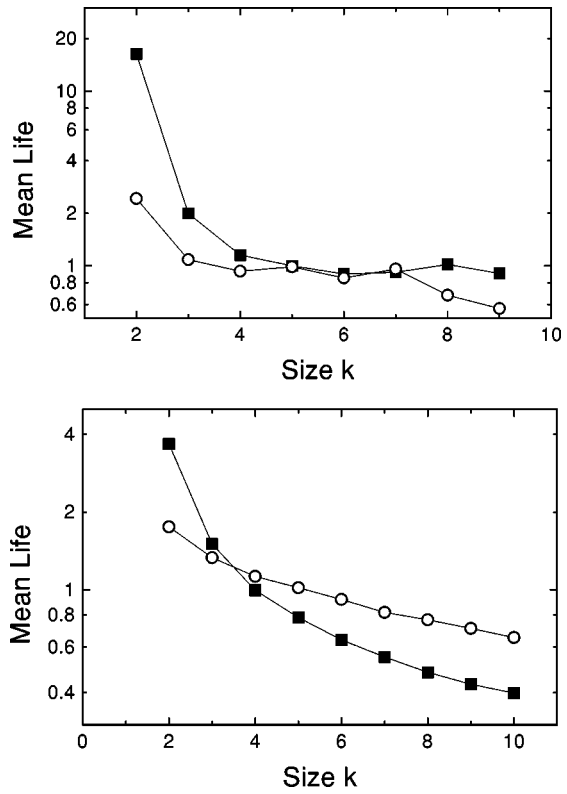

FIG. 3. The mean lives for clusters of different size k shown as a function of k. The solid squares (open circles) correspond to energetic (geometric) clusters. Lines are drawn to help visualization. The two sets correspond to the simulations described in Table I.

$$\tau = 1/Q'(0), \tag{21}$$

which can be calculated approximating $Q(t)$ by a polynomial near $t=0$. It is seen that mean lives decrease with cluster size because the absorption cross section increases and evaporation is easier.

The mean life of small clusters is larger for energetic than for geometric clusters. This is so on the one hand because evaporation is less likely when particles are bound (energetic clusters) and on the other because not every collision produces a size change since they are bound particles. Clusters tend to keep their identity.

For larger clusters the relation is the opposite due to a characteristic of the energetic clusters: due to energy fluctuations it becomes more and more probable that a particle belonging to the cluster gets enough energy to become unbounded from its neighbors. Such processes will usually occur deeply in the bulk of the cluster but they are counted as evaporation processes and therefore they are the end of the present cluster, even though the particle will, most likely, be reabsorbed a short time afterwards. Even though these processes have no physical implications their effect is to lowering the mean life of large energetic clusters. Further, this implies that, for energetic clusters, the mean life approaches a constant as density goes to zero.

B. Branching ratios

The branching ratios can be calculated using expression (15) written in terms of the accumulated probabilities $Q_\ell(t)$,

$$f_\ell = \frac{Q'_\ell(0)}{Q'(0)}, \tag{22}$$

that is, calculated in the same fashion as the mean life was.

Figures 4 and 5 show the branching ratios for all modes, for clusters defined geometrically and energetically, respectively, for sizes from 2 to 10. Due to the mode classification, for each value of k the graphs are divided in two regions, the fissions are plotted from $\ell=1$ to $\ell=k-1$ and the fusions from $\ell=k+1$ upwards. The mode $\ell=k$ is empty because there is no simple fusion or fission where the final cluster has the same size as the original one. For energetic clusters, the nonclassified transitions (for example, substitutions) are kept in mode $\ell=0$.

Simple fusions show an exponential decay because another cluster is needed to collide with the original one (of size k). The probability of the occurrence of such a collision is roughly proportional to the population of k-clusters, and it decays exponentially with k.[17,3,4]

Fissions are less probable as $k-\ell$ increases because to produce a smaller cluster it is necessary to evaporate a larger sub-cluster and this becomes more improbable as the subcluster increases in size. For energetic clusters, the nonclassified processes represent up to 7% of all cases.

From all the above it should now be clear that the standard hypothesis in the HNT that ''the only possible processes are evaporation and absorption of monomers ($\ell=k-1$ and $\ell=k+1$)'' is not really true. These monomer re-

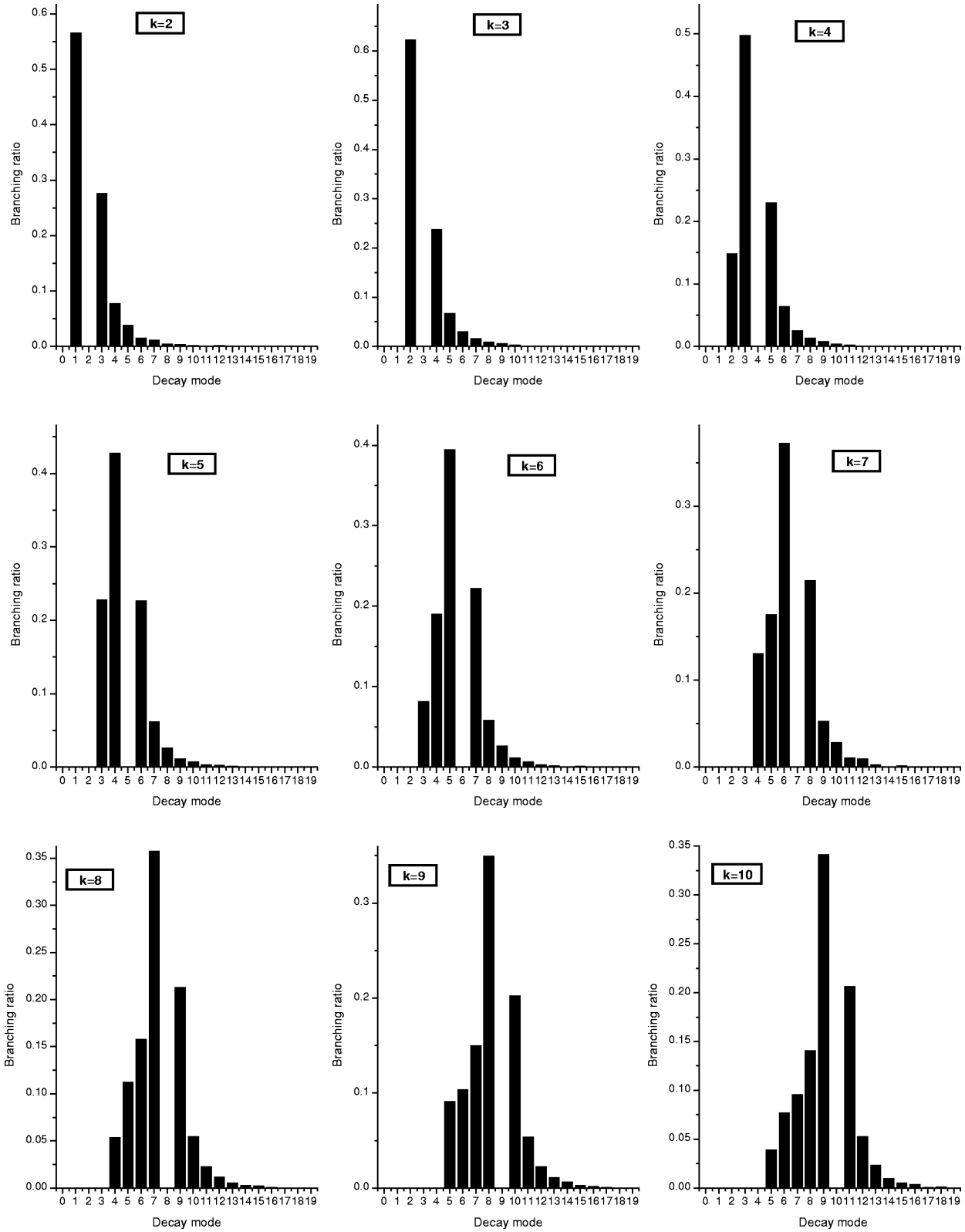

FIG. 4. Branching ratios of *geometric clusters* for the modes described in the text. The different graphs correspond to clusters of sizes from $k=2$ to $k=10$. The density and temperature values are those of simulation 2 in Table I. The other simulation in Table I shows qualitatively similar results.

lated processes are the most probable ones but the dynamical relevance of the other modes is not at all negligible. In order to measure the relative importance of the discarded processes, we define the probability of evaporation f_{evap} and absorption f_{absor} as the probability that a given cluster evaporates or absorbs another cluster regardless of the final size. That is, for clusters of size k, we define

$$f_{\mathrm{evap}}=\sum_{\ell=1}^{k-1} f_{\ell}, \tag{23}$$

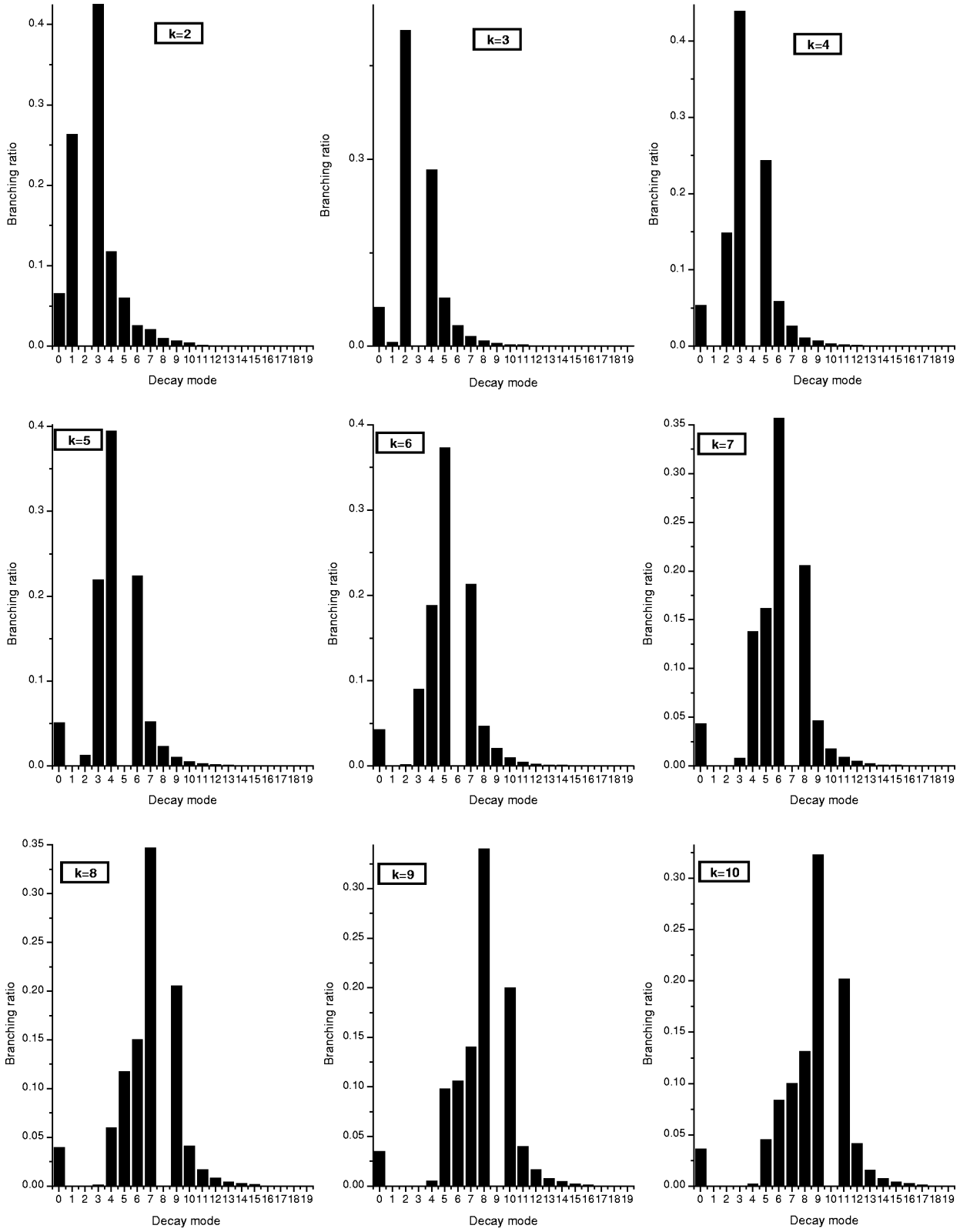

FIG. 5. Branching ratios for *energetic clusters* for the modes described in the text. The different graphs correspond to clusters of sizes from $k=2$ to $k=10$. The density and temperature values are those of simulation 2 in Table I. The other simulation in Table I shows qualitatively similar results.

$$f_{\text{absor}} = \sum_{\ell=k+1}^{\infty} f_{\ell}. \tag{24}$$

Then, the relative importance of the classical modes is measured as f_{k-1}/f_{evap} for the evaporations and as f_{k+1}/f_{absor} for the absorptions and they should be essentially 1 if the standard HNT were correct. These fractions are given in Table II for different cluster sizes and simulations. In

TABLE II. The relative importance of absorbing a monomer compared to all possible absorption modes, f_{k+1}/f_{absor}, and the relative importance of evaporating a monomer compared to all possible evaporation modes, f_{k-1}/f_{evap}. The results are given for different geometric and energetic cluster sizes. The density and temperature values are those of the simulation number 2 in Table I. If the HNT hypotheses were valid, these ratios should be essentially one.

k	f_{k+1}/f_{absor} (energ.)	f_{k-1}/f_{evap} (energ.)	f_{k+1}/f_{absor} (geom.)	f_{k-1}/f_{evap} (geom.)
2	0.63	1.00	0.64	1.00
3	0.66	0.99	0.63	1.00
4	0.68	0.75	0.65	0.77
5	0.69	0.63	0.66	0.65
6	0.70	0.57	0.66	0.59
7	0.71	0.54	0.67	0.55
8	0.72	0.51	0.67	0.52
9	0.73	0.49	0.66	0.50
10	0.73	0.47	0.67	0.49

some cases, the discarded processes correspond to 50% of the total number of evaporation or absorption processes.

It is shown that the monomer absorptions are roughly 70% of the total absorption processes, independent on the cluster definition and size. Obviously this ratio should depend on density. It goes down as density increases due to the larger population of dimers, trimers and other clusters to fuse with the original one. The monomer evaporations correspond to the total number of evaporation processes for small clusters ($k=2,3$), but as size increases the relative importance of evaporating larger sub-clusters increases. From the simulational results one cannot infer the behavior to be expected for clusters approaching macroscopic size.

To the best of our knowledge these branching ratios have not been measured before (computationally or experimentally), and it is always assumed that the HNT hypotheses are valid. At this point we underline the opportunity given by computer simulation: it makes it possible to measure phenomena—unreachable to direct experiments—used in the theory, thus giving more reliable data for theoretical predictions. Table II shows that a basic assumption has to be modified in a homogeneous nucleation theory to incorporate other processes. The branching ratios so obtained can be used with the generalized reaction model given in Ref. 9 to make numerical predictions, but as it will be shown in the following analysis these models fail because of the non-Markovian character of the decay processes.

C. Transition rates

The transition rates $T_{\not}(t)$ and $T(t)$ are quite difficult to evaluate from the data since it is necessary to take second derivatives of the accumulated probabilities; see Eq. (16).

We have studied the transition rates associated to dimers breaking into two monomers, $T_{2\to 1+1}(t)$. The accumulated probabilities are fitted to rational functions from where the transition rates are calculated analytically. In Fig. 6 we present the transition rates as functions of time. It is clear from the plots that for both the geometric and energetic clusters, the transition rates are not constant, but in the geometric

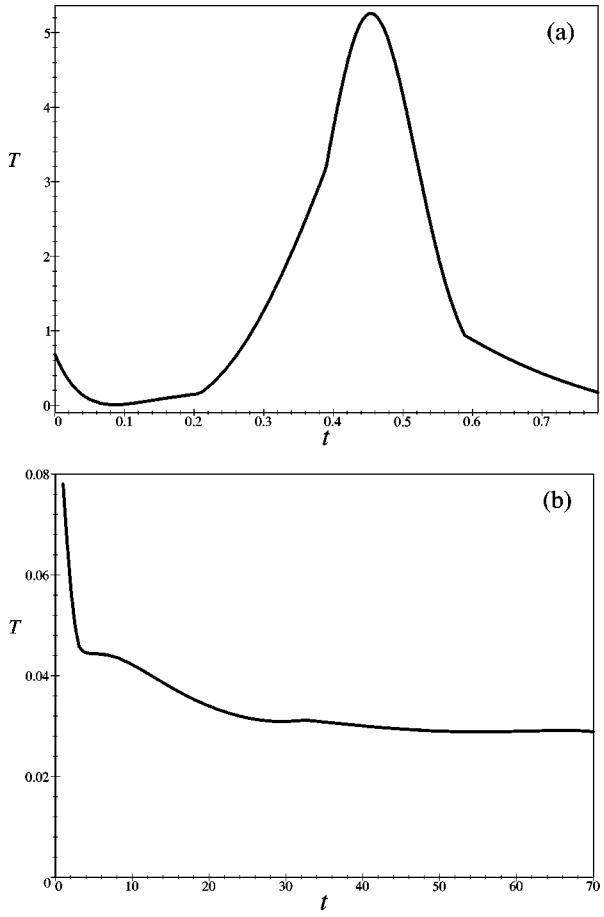

FIG. 6. The transition rate for the decay mode $2\to 1+1$ for both (a) geometric and (b) energetic clusters as measured in simulation 2. For the geometric clusters, the transition rate vanishes for $t>0.78$. As a reference, the dimer mean life for geometric clusters is $\tau=1.75$ and for energetic clusters $\tau=3.67$.

case the nonuniformity is more dramatic. The conclusion is that the decay processes are not Markovian contrary to another standard hypothesis of the usual HNT.

If a process is not Markovian, then clusters remember their time of creation, and memory effects must play a role. The origin of the memory effects is different for geometric than for energetic clusters.

For geometric dimers the memory effect comes from the fact that most of them correspond to two monomers colliding; thus the lifetime is quite short and has an upper limit determined by the collision parameters. Since the lifetime is bounded, the transition rate vanishes after a while.

The energetic dimers at first sight should have a constant transition rate because, by energy considerations, a third monomer is necessary to break the dimer. But, fast dimers collide sooner than slower ones, producing the effect that old clusters tend to be slower. As the probability for dimers to die depends on their average velocity, their transition rate is not constant. This effect is also present for geometric clusters, but the memory effect mentioned in the previous paragraph dominates.

For larger clusters the processes are not Markovian either. The absorption processes show a memory effect analogous to that described for energetic dimers, namely, faster

clusters collide first, thus producing that older clusters are, on the average, slower. The memory effect of the evaporation processes have a similar, but less dramatic, origin as in the case of the geometric dimers.

Besides—since fissions are endothermic and fusions are exothermic—newly born clusters have a different energy distribution function than clusters at equilibrium. Younger clusters created in a fusion will evaporate rapidly because they have more internal energy than the average. All these memory effects produce nonuniform transition rates and therefore birth–death processes are not Markovian. This prevents us from writing local-in-time equations for the evolution of cluster concentrations because, in a nonequilibrium situation, the memory effects imply that the dynamical equations depend on previous macroscopic states.

The memory effects are less notorious when energetic clusters are used because a large number of transitions corresponding to pure collisions are not counted, though other effects appear, such as complex decay modes and distortions of the velocity distribution functions.[23] The kinetic origin of memory effects come from dealing with clusters simply classified by their size without taking into consideration quite different dynamic characteristics (such as angular momentum or internal energy) between them. To have local equations, the clusters must be classified according to the values of their degrees of freedom, requiring a kinetic approach by means of kinetic equations.

V. CONCLUSIONS

In this article we have introduced a method that allows to obtain, from measurements in molecular dynamic simulations, the probabilistic properties of cluster decay processes. In particular, the method allows the calculation of the mean lives, branching ratios and, with more difficulty, the transition rates. Hence, these quantities needed in nucleation theories—which are usually modeled phenomenologically—are now obtained from our method.

The result of applying the method to a model two dimensional vapor (system of particles that interact with a square well potential) shows interesting results. First, it was shown that for two possible cluster definitions, the branching ratios do not coincide with the classical hypothesis that a cluster can only decay by means of absorbing or evaporating a monomer. The nonclassical modes represent, in some cases, up to 50% of the total decay events.

In all the simulations, the pressure was below saturation. But, in a nucleating vapor, where the pressure is higher, the concentrations of clusters increase, thus producing that the nonclassical modes will become more important. Therefore, in the study of a nucleating vapor, the HNT hypothesis are even less valid than in our simulations at equilibrium. As a consequence to produce a critical cluster in a supersaturated vapor, a cluster can change size in steps of size two or larger. Then, the nucleating rate can be radically different from the classical prediction.

Also, it was seen that the transition rates are not Markovian for neither the geometric nor the energetic definition, but for the latter the processes seem closer to being Markovian. This implies that out of equilibrium, it is impossible to write down local-in-time equations for the cluster populations.

The origin of the non-Markovian character of the decay processes comes from the coarse grain classification of clusters (labeling them by their sizes) and modes (labeled by the product sizes). Namely, since the reactions are classified without any mentioning of the dynamic degrees of freedom of the clusters involved much information is lost. It is known that if both classifications were more refined, the processes would be closer to being Markovian. In fact, in a complete description (leaving out no information whatsoever), as in a Liouville-like-equation for clusters, all processes would be Markovian. As soon as some information is lost equations become non-Markovian.[4,29]

Since it is far too difficult to write down and solve an exact (Liouville-like) equation for the vapor dynamics, an intermediate approach with a finer cluster classification scheme should be used. The kinetic approach consists in classifying clusters according to size, position, velocity and values of the internal degrees of freedom. With this approach, reasonably precise kinetic equations should be local in time even though strictly speaking one has to say that memory effects have rather short characteristic times.[30]

It should be noted that the numerical results obtained are valid for this specific model, and numerical differences are to be expected for other short range potentials. Possibly major differences should appear applying this method for three dimensional systems where, due to the larger connectivity, the surface tension is larger giving rise to more stable clusters.

ACKNOWLEDGMENTS

This work has been partially financed by *Fundación Andes Grant No. C-12971*. One of us (R.S.) also acknowledges *Fundación Andes* for financial support through grant No. C-12800 and *Fondecyt* Grant No. 295 0055. P.C. acknowledges his *Fondecyt* research Grant No. 197 0786.

[1] R. Beker and W. Döring, Ann. Phys. (Leipzig) **24**, 719 (1935).
[2] Y. B. Zeldovich, Acta Physicochim. URSS **18**, 1 (1943).
[3] F. F. Abraham, *Homogeneous Nucleation Theory* (Academic, New York, 1974).
[4] J. D. Gunton, M. San Miguel, and P. S. Sanhi, in *Phase Transitions and Critical Phenomena, Volume 8*, edited by D. Domb and J. L. Lebowitz (Academic, London, 1983), pp. 267–466.
[5] D. W. Oxtoby, J. Phys.: Condens. Matter **4**, 7627 (1992).
[6] P. Demo and Z. Kožisek, Phys. Rev. B **48**, 3620 (1993).
[7] D. Lippmann and W. C. Schieve, J. Phys. Chem. **97**, 3978 (1993).
[8] C. F. Wilcox and S. H. Bauer, J. Chem. Phys. **94**, 8302 (1991).
[9] K. Binder and D. Stauffer, Adv. Phys. **25**, 343 (1976).
[10] J. L. Katz and H. Wiedersich, J. Colloid Interface Sci. **61**, 351 (1977).
[11] J. L. Katz and M. D. Donohue, Adv. Chem. Phys. **40**, 137 (1979).
[12] V. I. Kalikmanov and M. E. H. van Dongen, J. Chem. Phys. **103**, 4250 (1995).
[13] G. W. Adams, J. L. Schmitt, and R. A. Zalabsky, J. Chem. Phys. **81**, 5074 (1984).
[14] R. Strey, P. E. Wagner, and T. Schmeling, J. Chem. Phys. **84**, 2325 (1986).
[15] A. Kacker and R. H. Heist, J. Chem. Phys. **82**, 2734 (1985).
[16] C. Hung, M. Krasnopoler, and J. L. Katz, J. Chem. Phys. **92**, 7722 (1990).
[17] R. Soto and P. Cordero, Phys. Rev. E **56**, 2851 (1997).
[18] K. Binder, D. Stauffer, and H. Müller-Krumbhaar, Phys. Rev. B **12**, 5261 (1975).
[19] H. Furukawa and K. Binder, Phys. Rev. A **26**, 556 (1982).

[20] F. H. Stillinger, J. Chem. Phys. **38**, 1486 (1963).
[21] H. Reiss, J. L. Katz, and E. R. Cohen, J. Chem. Phys. **48**, 5553 (1968).
[22] H. Reiss, A. Tabazadeh, and J. Talbot, J. Chem. Phys. **92**, 1266 (1990).
[23] R. Soto and P. Cordero, J. Chem. Phys. **56**, 8989 (1998).
[24] R. Soto and P. Cordero, Physica A **257**, 521 (1998).
[25] M. Marín, D. Risso, and P. Cordero, J. Comput. Phys. **109**, 306 (1993).
[26] M. P. Allen and D. J. Tildesley, *Computer Simulation of Liquids* (Oxford Science Publications, Oxford, 1987).
[27] D. C. Rapaport, J. Comput. Phys. **34**, 184 (1980).
[28] J. Ibsen (private communication).
[29] D. J. Evans and G. P. Morris, *Statistical Mechanics of Nonequilibrium Liquids* (Academic, London, 1990).
[30] R. L. Liboff, *Introduction to the Theory of Kinetic Equations* (Wiley, New York, 1969).